



Case Study

Analysis of a 3D Printed Heat Exchanger Using Ansys Discovery Software: Heat Convection Analysis

Authors: Andi Zhao, Syed Fuzail Ferhan, and Andrew Gryguć from the University of Waterloo IDEAs Clinic

Edited by János Plocher from the Ansys Academic Program

education@ansys.com

Ansys Software Used

This resource uses Ansys Discovery™ 3D product simulation software.

Summary

This case study explores the design, testing, and simulation of a 3D-printed cross-shaped heat exchanger using Ansys Discovery software. It provides a comprehensive overview of heat transfer principles, focusing on convection and conduction within a copper-filled PLA structure. The resource details experimental setup and procedures for measuring inlet/outlet temperatures and flow rates, followed by computational fluid dynamics (CFD) simulations to visualize conjugate heat transfer and flow behavior. It emphasizes the importance of accurate boundary conditions, material property estimation, and mesh refinement for reliable simulation results. Additionally, the study identifies potential sources of discrepancy—such as porosity, turbulence, and geometric tolerances—and discusses strategies for improving design efficiency. This resource serves as an experiential learning tool for students and engineers, bridging theoretical concepts with practical applications in thermal-fluid system design and optimization.

Table of Contents

1. Introduction.....	4
2. Theory	5
2.1 Principle of Heat Convection:	5
2.2 Real life application:	5
3. Experimental Apparatus.....	6
3.1 Heat exchanger.....	6
3.2 Faucet adapter.....	6
3.3 Flow restricter	6
3.4 Hair dryer adapter	7
3.5 Additional Equipment.....	7
4. Experimental Procedure	7
5. Experiment Result	9
5.1 Inlet and outlet temperatures and flow rates	9
5.2 Heat Exchanger thermal properties	10
6. Simulation Setup	13
7. Simulation Result.....	17
7.1 Conjugate Heat Transfer and Flow Visualization	17
7.2 Potential Sources of Error.....	18
7.2.1 Porosity Induced Leaking:.....	18
7.2.2 Heat Loss Through Air Convection and Water Evaporation:	19
7.2.3 Non-uniform Fluid Flow:.....	19
7.2.4 Experimental errors	19
7.2.5 Geometric tolerances	19
7.3 Next Steps and Recommendations.....	19
8. Conclusion & Summary	20

1. Introduction

Heat exchangers are vital components in a wide range of industrial processes, enabling efficient transfer of thermal energy between fluids in applications such as power generation, chemical processing, refrigeration, and automotive systems. Their performance directly influences energy efficiency, process reliability, and operational costs across industries. Designing an effective heat exchanger requires careful consideration of thermal performance, fluid dynamics, material selection, and fouling behavior. This case study investigates thermal energy transfer between two fluids using a 3D-printed cross-shaped heat exchanger (Figure 1), designed with separate air and water channels. The experimental setup involves coupling a water stream and a heated air stream, with inlet and outlet temperatures recorded once steady-state was reached. The setup demonstrates how conduction and convection interact in real systems. While convection serving as the dominant mechanism of heat transfer in this application, arising from fluid movement through the channels, conduction occurs within the solid copper-filled PLA walls of the exchanger.

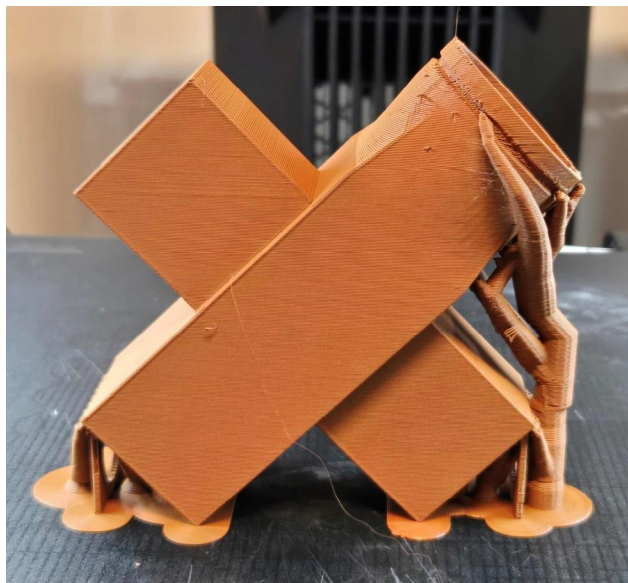


Figure 1: Image of 3D-printed Heat Exchanger for Experiments

To optimize these systems and reduce development costs, simulation and computational modeling have become essential tools. Numerical simulation allows engineers to predict temperature distribution, pressure drops, and heat transfer rates under various operating conditions—long before physical prototypes are built. Thus, this case study complements the experiments with a conjugate heat transfer simulation in Ansys Discovery that is verified with the experimental data. This allows for visualization of the physical phenomena and the changes in temperature, heat flux and velocity within the heat exchanger which are difficult or impossible to see in the experiment.

Beyond resolving measurement fallacies, this case study extends naturally into a design optimization challenge. Students can evaluate trade-offs between maximizing heat transfer and minimizing pressure losses caused by back-pressure; this mirrors the multi-objective nature of real-world thermal–fluid system design, where engineers must balance efficiency with practical constraints such as flow resistance, material selection, and manufacturing feasibility.

Ultimately, the project demonstrates how combining low-cost prototyping, hands-on experimentation, and Ansys Discovery simulations provides a powerful experiential learning platform. It not only reinforces theoretical heat transfer concepts, but also trains students to think critically about boundary conditions, validation, and design trade-offs, key skills for modern engineering practice.

2. Theory

2.1 Principle of Heat Convection:

Heating by convection is the process of transferring heat through the movement of fluids. The movement can be natural for example having warmer and less dense fluids to rise or this behavior can be forced externally using pumps. Efficient convection heating relies on the strategic placement of heat sources to maximize airflow and heat distribution. The method of convection combines two mechanisms which are random molecular motion and bulk fluid motion which carries heat away from or towards the surface.

2.2 Real life application:

Heat convection is commonly used to control temperature in systems such as air conditioners, central heating systems, convection ovens use hot air to cook food (air fryers also use the same method), car radiators (which use louvered fins which is the most effective shape for heat exchange (reference paper on teams)) use flowing coolant for heat exchange in order to maintain engine temperature and heat exchangers are used in countless industrial processes such as power plants in order to transfer heat from one fluid to another effectively (see Figure 2). Hot air balloons also use convection, when the air is heated it becomes less dense thus it rises, the created convection currents are what lift the balloon. For more information on convection as well as conduction and radiation, the reader is kindly referred to: [Introduction to Heat Transfer with Ansys Discovery.](#)



Figure 2: Convection example of a convection oven and a car radiator

3. Experimental Apparatus

Figure 3 shows the experimental setup, with details of the main components below.



Figure 3: Heat exchanger experimental setup

3.1 Heat exchanger

The heat exchanger was fabricated using a copper-filled PLA filament, and its thermal conductivity, density, and specific heat capacity were approximated through additional material testing. As presented in Figure 3, the heat exchanger is cross-shaped and has two overlapping but independent channels, in which the larger channel is for running through water and the smaller one is for running through air; a TPU buffer is connected to the circular end of the water channel to allow more convenient connection with the faucet adapter and prevent the brittle heat exchanger model from fracturing when forcing the adapter onto the fragile circular end.

3.2 Faucet adapter

As shown in Figure 3, the faucet adapter (part with the arrow pointing to the right) has a near frustum appearance with the larger end threaded; the threaded end shall connect to the threaded TPU buffer tightly to achieve acceptable water tightness, and the smaller end shall fit onto a water faucet using 1 mm 'O' rings.

3.3 Flow restricter

As shown in Figure 3, the flow restricter (part with the arrow pointing to the left) can be installed onto the rectangular end of the water channel to allow water to occupy the entirety of the water channel by restricting the exiting water flow.

3.4 Hair dryer adapter

As shown in Figure 3, the hair dryer adapter (arrow pointing down) has a rectangular end and a more complex circular end; the rectangular end shall be fit onto one end of the air channel, and the circular end shall connect with the hairdryer.

3.5 Additional Equipment

To collect the experimental data the following equipment was used.

- Anemometer
- Thermal couple for air and water applications
- Hair dryer
- Water faucet
- 1 mm 'O' rings
- Watertight container of adequate size
- A scale
- A timer

4. Experimental Procedure

The experimental setup began with the mechanical assembly of the heat exchanger. The faucet adapter was connected to the circular inlet, the flow restricter was attached to the larger rectangular outlet, and the hairdryer adapter was affixed to the smaller rectangular outlet and reinforced using hot glue to ensure a secure seal (Figure 4).

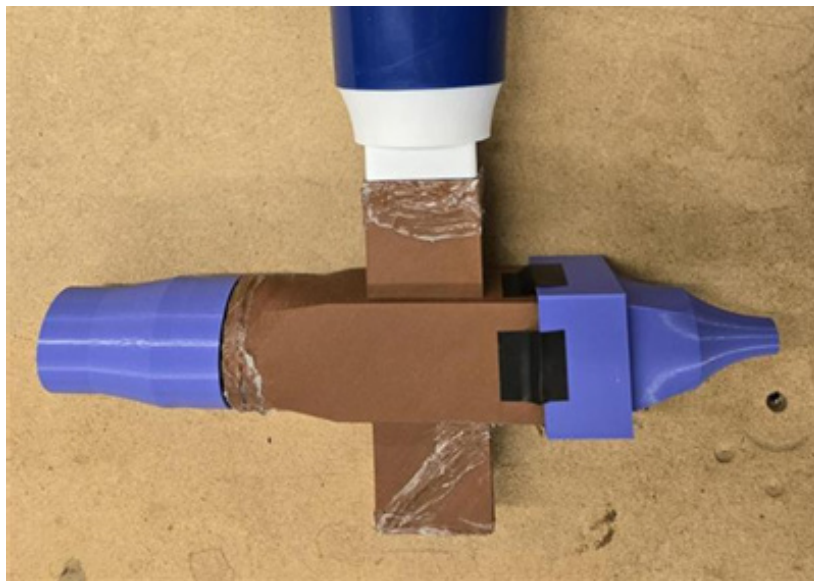


Figure 4: Assembled heat exchanger.

To calibrate the water flow, the heat exchanger was held beneath an open faucet without direct attachment. The faucet was gradually opened until the internal channel of the heat exchanger filled completely without causing overflow at the adapter. The corresponding lever position was marked for consistency in subsequent steps, and the prototype was then removed (Figure 5).



Figure 5: Water flow (no overflow at correct rate)

With the flow rate unchanged, a thermocouple was placed at the faucet outlet to measure the inlet water temperature. Simultaneously, the hairdryer was activated, and a second thermocouple was used to record the outlet air temperature (Figure 6).

To determine the water mass flow rate, an empty container was weighed and positioned to collect water from the faucet at the calibrated flow rate for a fixed duration. The container was then reweighed, and the mass difference was used to calculate the flow rate.

Next, the hairdryer was connected to the heat exchanger via the adapter, and the air outlet velocity was measured at the exchanger's exit. It was critical to avoid measuring directly at the hairdryer outlet to ensure accurate representation of the exchanger's performance.

Finally, the heat exchanger was connected to both the faucet and the hairdryer. Thermocouples were inserted into the drilled hole on the hairdryer adapter (air inlet) and at the air outlet channel. With the water and air flow rates maintained as previously determined, temperature readings at both air inlet and outlet were recorded over a defined period once steady-state conditions were achieved.



Figure 6: Demonstration of experimental apparatus

5. Experiment Result

5.1 Inlet and outlet temperatures and flow rates

Assuming the fluid flow is under steady state when the measurement is taken, the mass flow rate of the faucet and the hairdryer would be equal to the mass flow rate of the heat exchanger channel inlet. Although velocity is measured at the heat exchanger's outlet instead, the mass flow rate can be calculated using Formula 1:

$$\dot{m} = vA\rho$$

Formula 1: Mass Flow Rate Formula

Where:

- \dot{m} is the mass flow rate
- v is the fluid velocity
- A is the fluid cross section area
- ρ is the fluid density

Besides the velocity measurements, the water inlet and outlet temperatures were measured (see Table 1). Based on Formula 1, the mass flow rates of water and air were calculated. It must be noted that the initial assumptions treated the hairdryer's outlet flow rate as constant, but this ignored the back-pressure induced by the heat exchanger, which significantly reduced airflow. By revising the measurement approach, recording velocity at the exchanger outlet and adjusting density for temperature rise, researchers improved agreement between experiment and simulation (compare the below section on simulation results) and highlighted the strong influence of system constraints on performance.

Table 1: Heat exchanger test setup data with initial conditions.

Heat Exchanger Water Inlet \dot{m} (kg/s)	0.0725
Heat Exchanger Air Outlet Cross Section (m ²)	0.000567
Heat Exchanger Air Channel Inlet \dot{m} (kg/s)	0.00185
Heat Exchanger Water Inlet T (°C)	10
Heat Exchanger Air Inlet T (°C)	44

It is of note that the time at 0s is not the time when the trail begins, but a chosen time after the setup reaches steady state. In this scenario, time at 0s is 22 seconds into recording. As seen in Table 2, an average temperature drop of 20 °C has been observed at the center of the air outlet channel.

Table 2: Air inlet and outlet (stabilized) temperature measurements over time.

Time (s)	0	2	4	6	8	10	12	14	16	18	20	22	24	26	28	30	Avg
Air Inlet T (°C)	40.7	40.6	40.6	40.7	40.7	40.8	40.9	41.0	41.2	41.3	41.4	41.5	41.6	41.6	41.7	41.8	41.1 ±0.4
Air Outlet T (°C)	21.3	21.5	21.8	22.1	22	22.2	22.1	21.8	22.4	22.2	22.4	22.7	22.5	22.7	22.5	22.8	22.2 ±0.4

5.2 Heat Exchanger thermal properties

In order to run a realistic simulation in the next step, besides the physics condition measured in the setup, one also needs to apply the correct material properties as these define the conductive performance of the heat exchanger. In Ansys Discovery, users can choose from a range of different materials, however, as this is a specific copper-infused FDM-printed filament (for an overview on different print processes, the reader is referred to Additive Manufacturing Processes | Education Resources), a new user defined material should be used.

As seen in Figure 7, the three essential thermal material parameters of a solid are its density, thermal conductivity coefficient, and the specific heat capacity to allow thermal and fluid dynamics computation.

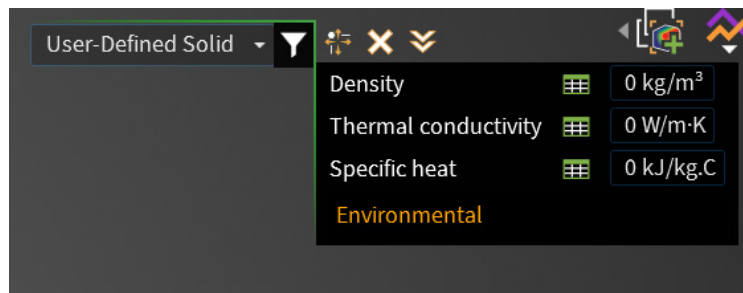


Figure 7: User-defined material card in Ansys Discovery tool highlighting the fields for key thermal properties.

The density of the copper like filament material is 2300 kg/m³ according to the filament developer, and the specific heat of a homogeneous composite material can be calculated by summing up the specific heat of each constituent as pure substances weighted by their composition in the composite material. The filament used in prototyping consists of two major materials, which are pure copper and

standard HTPLA. Thus, its specific heat can be described by Formula 2:

$$C_{p_filament} = \left(\frac{m_{PLA}}{m_{filament}} \right) C_{p_PLA} + \left(\frac{m_{Cu}}{m_{filament}} \right) C_{p_Cu}$$

Formula 2: Specific heat formula for compound

Where:

- $C_{p_filament}$ is the heat capacity of the filament
- C_{p_PLA} is the heat capacity of the HTPLA portion of the filament
- C_{p_Cu} is the heat capacity of the copper portion of the filament
- m is the mass of each material

Since the specific heat of copper is 395J/kg·K, and the specific heat of HTPLA is 1800 J/kg·K, the specific heat of the composite filament with 60 wt.% copper and 40 wt.% HTPLA would be approximately 950 J/kg·K.

To approximate the thermal properties of the copper filled composite PLA filament, which was not specified by the vendor, three specimens were manufactured at 100% infill density using the filament in question as shown in Figure 8. The specimens, which are an irregular tetrahedron, a semi sphere, and a regular tetrahedron, were placed on top of a heat bed that was preheated to 50 °C. The temperature change of the specimens shown in the cameras display after 10 minutes were then captured by a thermal camera.



Figure 8: Measurement of the surface temperature of the 3D-printed test specimen made of copper filled HTPLA using a thermal camera.

By plotting the data points collected from respective specimen relative to time, it can be discovered that a majority of the data follow a logarithmic trend. The similar specimen-on-bed setup is replicated in Ansys Discovery software with a monitor created on the spot where the temperature has been observed in the experiment. A time vs. temperature plot of the simulation results can be obtained by running the simulation with arbitrary material thermal properties. By tuning the heat loss through air and the thermal conductivity coefficient on a trial-and-error basis, a plot that fits into the logarithmic trend of the experimental data is obtained as shown in Figure 9. Most curves plateau at below 45 °C

except for the irregular tetrahedron. Eventually, it is approximated that the actual thermal conductivity coefficient of the 3D printing filament lies around 0.7 WmK , which constitutes the simulation curve in Figure 10.

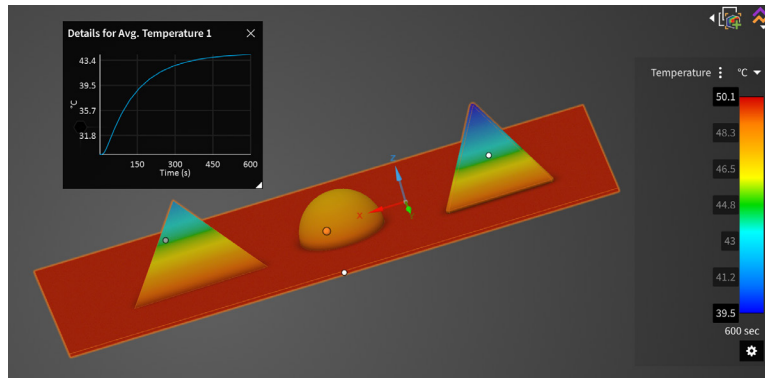


Figure 9: Transient heat transfer simulation of a irregular tetrahedron, a semi sphere, and a regular tetrahedron on the heated print bed.

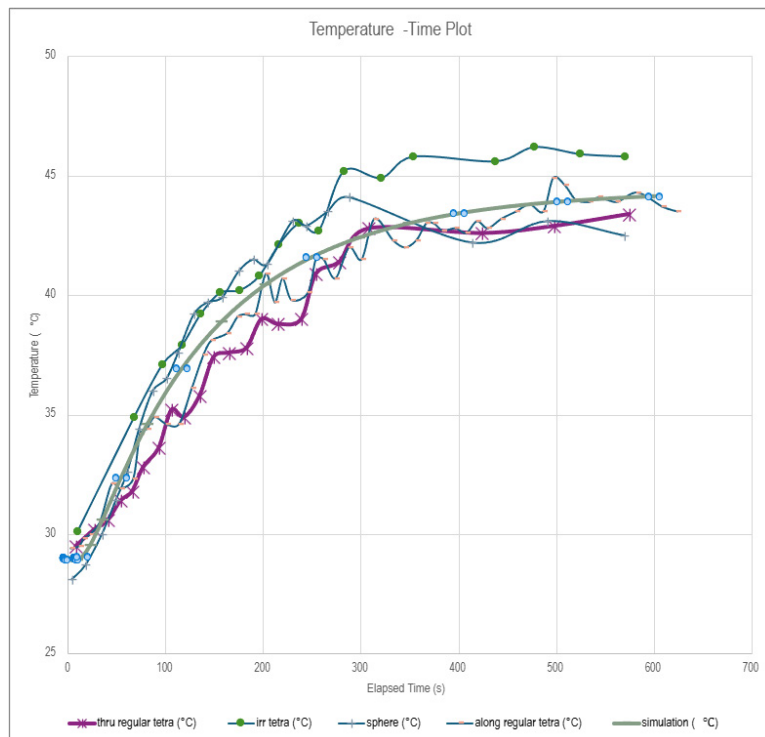


Figure 10: Change of surface temperature overtime of different copper filled composite filament specimens heated by a print bed set to 50°C and compared with the simulation results of the same.

6. Simulation Setup

Starting from the heat exchanger CAD geometry (see attached files), the fluid domain for water and air must be defined. This was done using the Volume Extract tool in the prepare tab of Ansys Discovery, as shown in Figure 11.

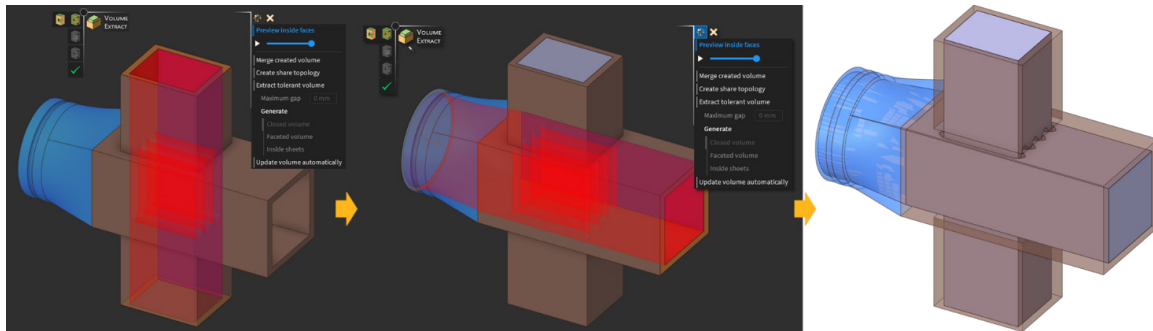


Figure 11: Extraction of two fluid domains from the heat exchanger.

Next, inlet (green) and outlet (orange) flow boundary conditions were defined for the air and water streams, selecting the opposing surfaces of the fluid domains, as shown in Figure 12.

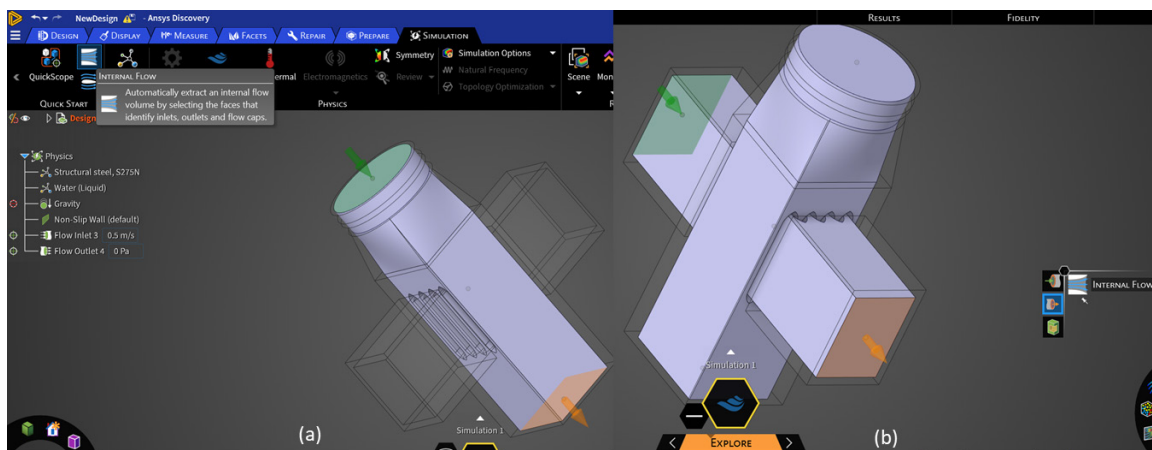


Figure 12: Internal Flow button location

Subsequently, the inlet boundary condition was changed from the default “velocity” to “mass flow rate” (see Figure 13) and the value were set as experimentally determined (compare Table 1). Likewise, the fluid temperatures were set after activating those in the flow inlet heads-up display (indicated by the thermometer shaped icon) .

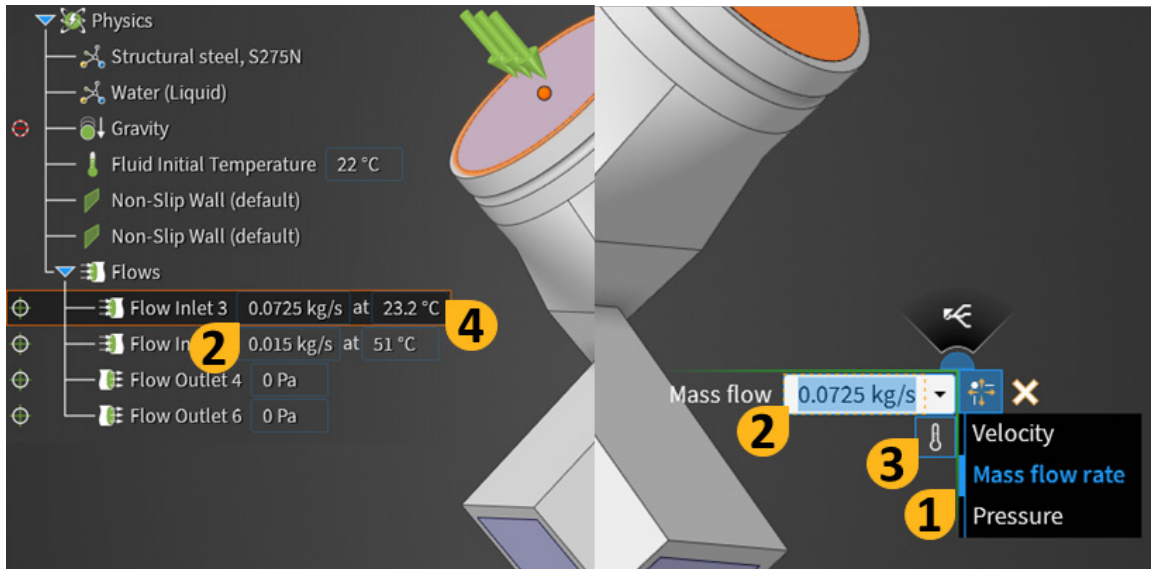


Figure 13: Defining the mass flow rate either from within the Physics tree (left) or the Inter Flow tool in the heads-up display of Ansys Discovery.

In order to account for convective heat transfer around the heat exchanger, a solid thermal convection boundary condition was added (see Figure 14), representing the experimental environment conditions, i.e. $10 \text{ W/m}^2\cdot\text{°C}$ at a temperature of 22°C .

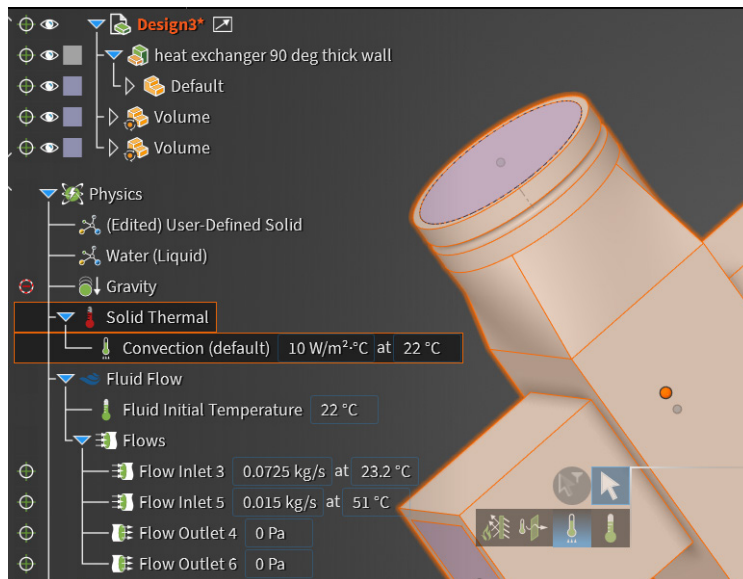


Figure 13: Convection boundary conditions and input values.

By default, Ansys Discovery assigns solid components “Structural Steel”; thus, this was changed to Cu-infused PLA, using a user-defined solid (see section above) with material density, thermal conductivity coefficient, and specific heat capacity, set to 2300 kg/m^3 , $0.7 \text{ W/m}\cdot\text{K}$, and $0.951 \text{ kJ/kg}\cdot\text{°C}$, respectively. Similarly, for fluid flow simulations Ansys Discovery assigns fluid components “Water”; thus, the air channel was selected and assigned the medium “Air Gas” (see Figure 15).

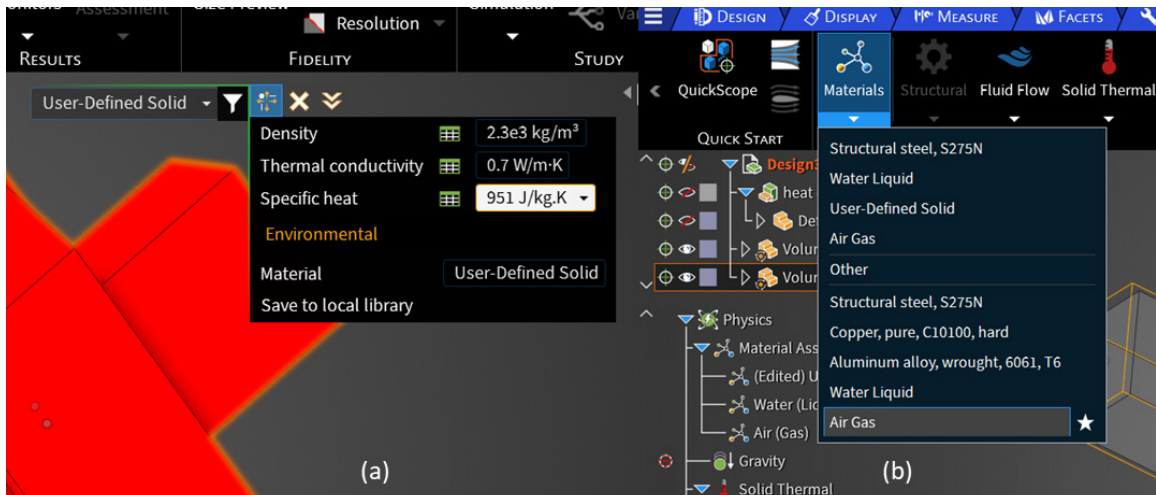


Figure 15: (a) User-defined material definition for the copper-filled PLA with the thermal properties filled in on the heads-up display and (b) material settings in the simulation tab with recently used materials.

Two construction planes were added parallel to the air inlet and outlet faces and subsequently move inwards, cutting the fluid domain (see Figure 16). These are used to apply monitors to, recording the average inlet and outlet temperature.



Figure 16: Monitors applied to construction planes cutting the air fluid domain near the inlet and outlet.

When performing CFD analysis, ensuring sufficient mesh resolution across small geometric features is critical for accuracy. The mesh needs to be fine enough to resolve gradients in velocity, temperature, and other relevant variables, especially near walls and in regions with high curvature or small gaps. In this heat exchanger example, a mesh size of 0.4 mm was used but in order to better resolve the

central fins where gradients are expected to be large, a local mesh refinement of 0.2mm was added (see Figure 17).

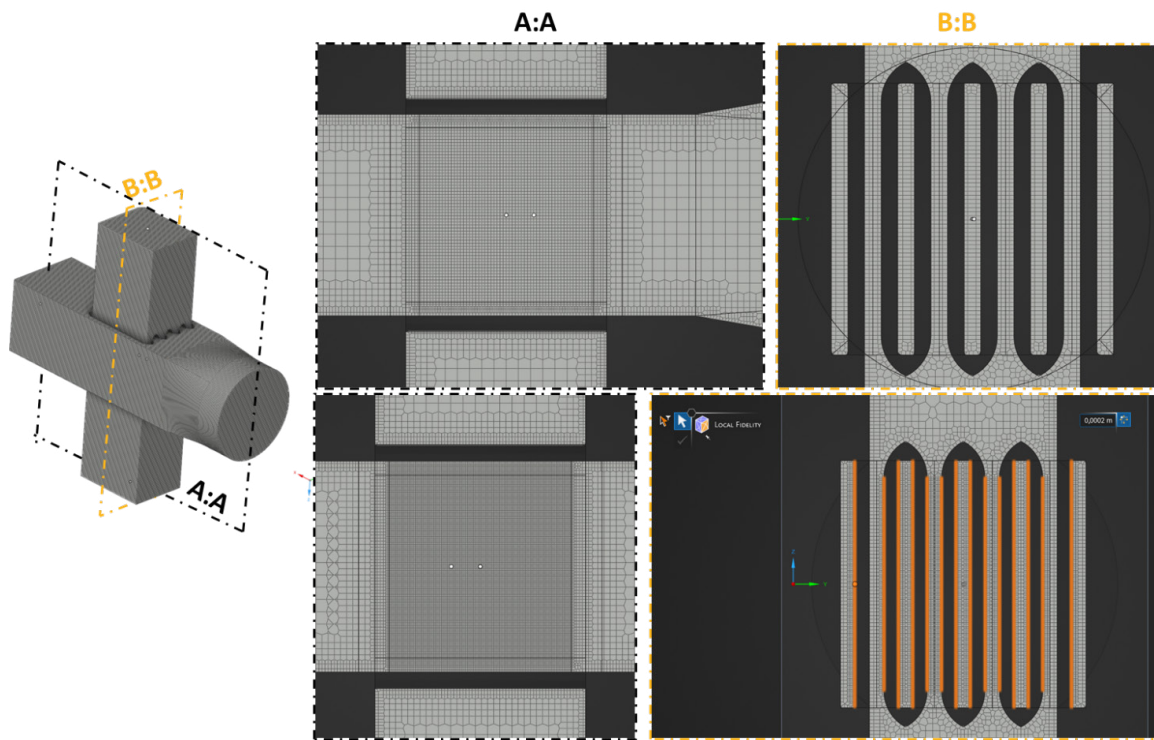


Figure 17: Meshed heat exchanger without local mesh refinement (top row) and with local mesh refinement (bottom row).

7. Simulation Result

7.1 Conjugate Heat Transfer and Flow Visualization

Besides the quantitative comparison of the experimental results, Ansys Discovery allows for a qualitative analysis, i.e. the visualization of the internal flow (impossible through experiments) and supports the understanding of the inner workings of the heat exchanger, allowing for to make informed decisions about how it can be improved to make it even more efficient.

As shown in Figure 18, an average temperature drop of around 10 °C has been observed with the boundary conditions presented in the screenshot. However, taking the average across the plane may not precisely and accurately address the complex turbulent behavior at the air outlet channel, which could be one of the contributing factors to the 10 °C deviation between the experimental data and the simulation results. In the next section more potential sources of error are discussed.

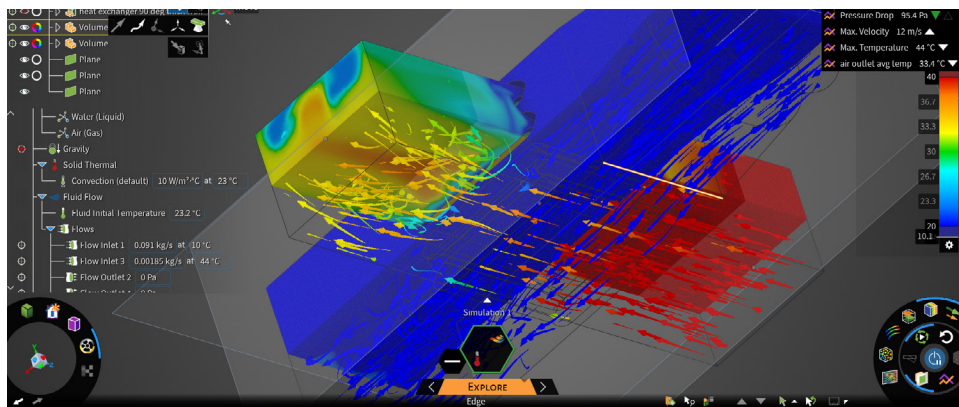


Figure 18: Simulation result showing the temperature distribution using contours and vectors.

As seen in Figure 19, the iso-surface at 33.4 °C is distributed non uniformly across the air outlet. Although the lack of precision in data collection methods can play a role in inconsistencies between experimental values and expected values.

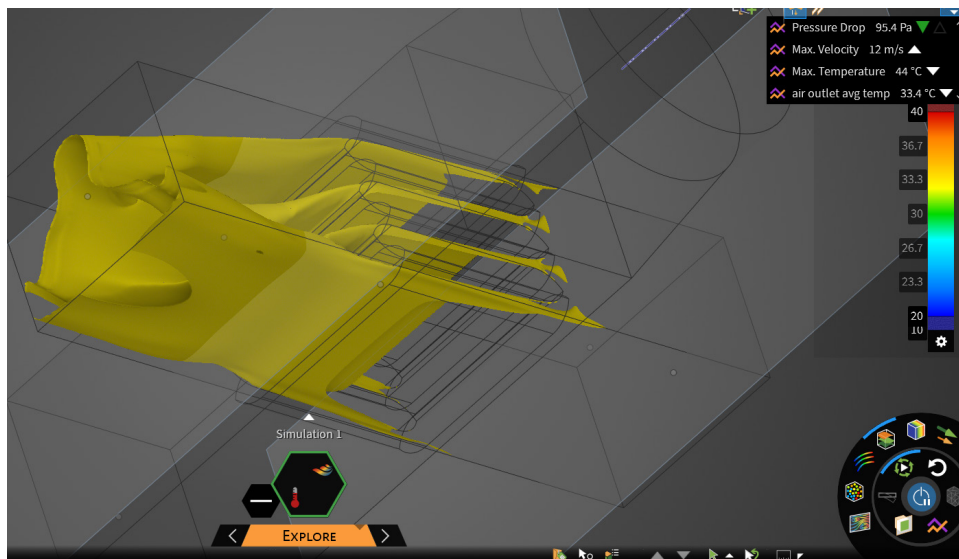


Figure 19: Temperature iso-surface at 33.5 °C.

The air outlet channel velocity side view and top view depicted by Figure 20 show that fluid behaves similar to a venturi tube after exiting the heat transfer zone. The compressed high-speed air collides into near stagnant air and produces sophisticated turbulent behavior as well as complex temperature distributions.

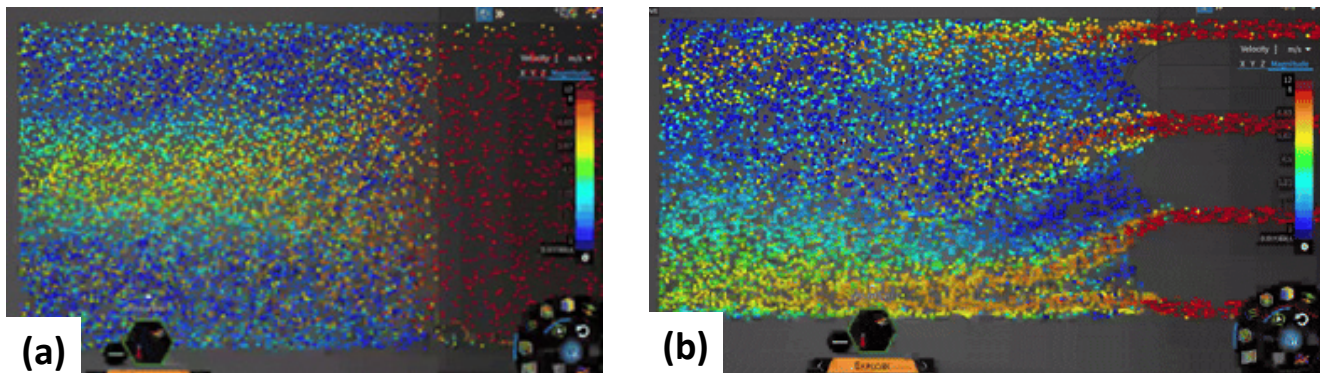


Figure 20¹: Air outlet channel (a) top view and (b) side view

As shown by Figure 21, two large eddies form on the top and the bottom sides of the channel after high-speed air has been ejected from the thin gaps. While a significant amount of mixing has made the fluid streams less distinguishable by the end of the channel, a relatively stable vertex can be observed at the center of the channel.

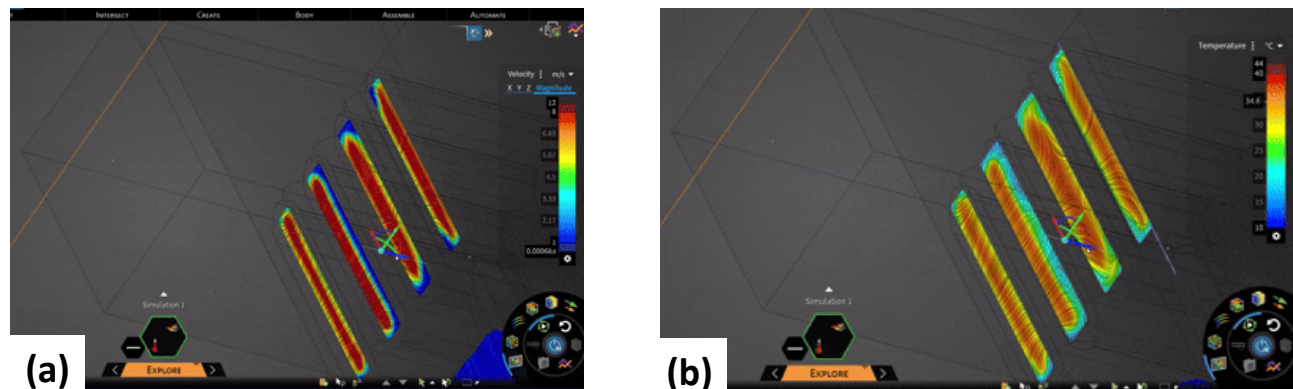


Figure 21: (a) Velocity and (b) Temperature of air at outlet

7.2 Potential Sources of Error

Experimental measurements showed an average 20 °C temperature drop between the heated air inlet and outlet (see Table 2), while simulations predicted around a 10 °C drop. The discrepancy was attributed to turbulence, porosity-induced leakage, evaporative cooling, and experimental uncertainties such as thermocouple placement. Computational fluid dynamics (CFD) revealed non-uniform outlet temperature fields, eddy formation, and turbulent flow structures similar to venturi effects; these provided insight into why perfect agreement was not achieved. These aspects will be discussed in the following.

7.2.1 Porosity Induced Leaking:

The heat exchanger prototype is manufactured through FDM 3D printing. By extruding layers of material on each other, microscopic defects are inevitability considering the high temperature requirements of the copper filament. These defects are what allow for both fluids to be in direct contact which impacts the results along with the air flow. This explains the lower temperatures measured in the experiment.

¹ To see a GIF of Figures 20 and 21, open the Word Document included in this resource download.

7.2.2 Heat Loss Through Air Convection and Water Evaporation:

There may be ambient air backflow occurring at the end of the air outlet channel in the experiment, which will cause the near boundary temperature measurements to be significantly lower than expected. Cold water trapped within the solid model is also able to absorb excessive latent heat before evaporating, further cooling down the air more than it normally should during the process. Consequently, the higher outlet temperature obtained by the simulation seems reasonable.

7.2.3 Non-uniform Fluid Flow:

Sophisticated turbulent behavior has been observed at the air outlet channel of the heat exchanger. The turbulence model used in the simulation setup (k- ω SST) only generates an approximation of the turbulent behavior in a more idealized situation, which subsequently causes inconsistency in temperature simulation results compared to the experiment. Moreover, FDM prints have a very rough surface exacerbating this effect, while the numerical model considered perfectly smooth surfaces.

7.2.4 Experimental errors

During the first two iterations of the experiment the data collected was unreliable as the water temperature was not allowed to reach a constant temperature which was addressed by allowing the water to run until it reached a constant temperature of 10 °C.

The placement of the thermocouple was also another key source of error, the thermocouple was placed halfway through the air inlet to measure the temperature can disrupt the fluid flow which in turn would negatively impact the measurements. The use of monitors in the simulation do not interfere with the measurement and this provide a more consistent and reliable data tracking.

The information which was provided the by the filament manufacturer was limited and calculated material properties could vary significantly due to inconsistencies in test prints and methods used. For example, a denser material can transfer heat more efficiently because molecules are more closely packed. Another material property which couldn't be verified was the specific heat capacity, a higher specific heat capacity allows the material to store more heat rather than transferring it in turn leading to slower temperature changes.

7.2.5 Geometric tolerances

While finding reasons behind the discrepancies between the experimental and simulated values it was noted that the cross-sectional area of the air outlet was 0.000595 m² in the simulation model whereas it was 0.000567m² in the experimental model. A larger outlet allows for an increased air flow rate which in turn leads to a lower change in temperature as the air spends less time interacting with the cooler bit which can explain any discrepancies.

7.3 Next Steps and Recommendations

A key lesson in this case study is that the air mass flow rate is not fixed but strongly shaped by the boundary conditions of the system. The initial method estimated flow from the hairdryer by measuring outlet velocity, multiplying by the outlet area, and applying ambient air density. While valid in isolation, this ignored the induced back-pressure created when the heat exchanger was attached, which restricts flow and lowers the effective mass flow rate. The revised approach instead measured velocity at the heat exchanger outlet, using the correct channel cross-sectional area and adjusting air density for elevated temperature. This boundary-aware methodology produced far better agreement between

experiment and simulation, showing how system constraints must be embedded in flow predictions. Importantly, the case study can extend beyond measurement accuracy into a design optimization challenge. Rather than focusing only on maximizing heat transfer, students can examine trade-offs between thermal performance and pressure loss minimization, reflecting the multi-objective balance required in real-world thermal–fluid design.

8. Conclusion & Summary

We can see that there are some differences between the measured values and the simulated values, which is likely to do with porosities in the print, measurement difficulties and experimental errors and some assumptions and simplification that were made in the simulation; however, both simulation and measurement do show that heat is being transferred between the two fluids without any direct contact. By using Ansys the team was able to see possible reasons for errors and other reasons behind a less efficient heat transfer such as the generation of Eddies and many other possible sources as mentioned previously in the sources of error section. The ability to literally look into the heat exchanger through the use of simulation opens up a whole new level of learning through the power of visualization.

© 2025 ANSYS, Inc. All rights reserved.

Use and Reproduction

The content used in this resource may only be used or reproduced for teaching purposes; and any commercial use is strictly prohibited. The full Academic Terms & Conditions can be found [using this link](#).

Document Information

This case study is part of a set of teaching resources to help introduce students to topics related to fluids.

Ansyes Education Resources

To access more undergraduate education resources, including lecture presentations with notes, exercises with worked solutions, microprojects, real life examples and more, visit www.ansys.com/education-resources.

Feedback

Here at Ansys, we rely on your feedback to ensure the educational content we create is up-to-date and fits your teaching needs.

[Please click the link here](#) out a short survey (~7 minutes) to help us continue to support academics around the world utilizing Ansys tools in the classroom.

ANSYS, Inc.
Southpointe
2600 Ansys Drive
Canonsburg, PA 15317
U.S.A.
724.746.3304
ansysinfo@ansys.com

If you've ever seen a rocket launch, flown on an airplane, driven a car, used a computer, touched a mobile device, crossed a bridge or put on wearable technology, chances are you've used a product where Ansys software played a critical role in its creation. Ansys is the global leader in engineering simulation. We help the world's most innovative companies deliver radically better products to their customers. By offering the best and broadest portfolio of engineering simulation software, we help them solve the most complex design challenges and engineer products limited only by imagination.

visit www.ansys.com for more information

Any and all ANSYS, Inc. brand, product, service and feature names, logos and slogans are registered trademarks or trademarks of ANSYS, Inc. or its subsidiaries in the United States or other countries. All other brand, product, service and feature names or trademarks are the property of their respective owners.

© 2025 ANSYS, Inc. All Rights Reserved.